AIP Conference Proceedings

RESEARCH ARTICLE | MARCH 29 2012

On the development of an impact-loaded wedge test using ORVIS FREE

Marcia A Cooper; Wayne M. Trott

AIP Conf. Proc. 1426, 430–433 (2012)
https://doi.org/10.1063/1.3686310

ON THE DEVELOPMENT OF AN IMPACT-LOADED WEDGE TEST USING ORVIS

M. A. Cooper[1] and W. M. Trott[1]

[1]*P.O. Box 5800, Sandia National Laboratories, Albuquerque, NM, 87185*

Abstract. Experiments using a wedge-shaped explosive sample shocked with an attenuator-explosive booster are historically used to provide data for fitting an empirical relationship between the input stress and shock-to-detonation run distance. Recent problems with plane wave lens availability and increased needs for characterizing novel explosive formulations have highlighted the need for a modernized approach to traditional wedge tests. We present our concept of an impact-loaded wedge test which uses a gas gun, a wedge-shaped explosive sample and the line-imaging ORVIS (Optically Recording Velocity Interferometer System) diagnostic. The ORVIS optical configuration is modified from the standard configuration to project the laser line onto the inclined surface of the wedge-shaped sample where the return light is collected with a streak camera. Initial data of shock breakout in inert samples are presented.

Keywords: ORVIS, interferometry, impact: velocity.
PACS: 62.50.Ef, 07.60.Ly.

INTRODUCTION

Explosive wedge tests are used to generate a log-log plot of run distance to detonation for a given input pressure. Commonly known as a Pop-plot, it provides a means of comparison between different explosives (left image of Fig. 1). Historically, wedge tests have relied on explosive plane wave lenses and the proper use of attenuators (right image of Fig. 1). The plane wave lenses are often quite large with diameters of 8 inches and an experimental facility suitable for testing large quantities of explosives is required. Here we propose an Impact-Loaded Wedge Test that generates an incident planar shock in an explosive wedge with a gas gun projectile and measures the explosive response with our Optically Recording Velocity Interferometer System (ORVIS). The shock path and particle velocity data from the inclined surface are measured.

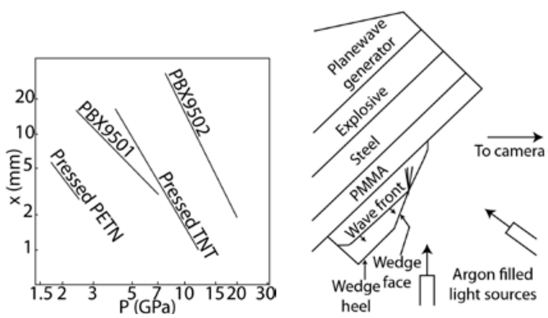

Figure 1. POP-plot with four common explosives (left) and a traditional wedge test arrangement [1] (right image).

ORVIS COUPLED TO THE EXPLOSIVE COMPONENT FACILITY'S GAS GUN

The single-stage gas gun at SNL's Explosive Components Facility (ECF) has an 18-meter long, 6.35-cm diameter barrel. Impact velocities range

Shock Compression of Condensed Matter - 2011
AIP Conf. Proc. 1426, 430-433 (2012); doi: 10.1063/1.3686310
2012 American Institute of Physics 978-0-7354-1006-0/$0.00

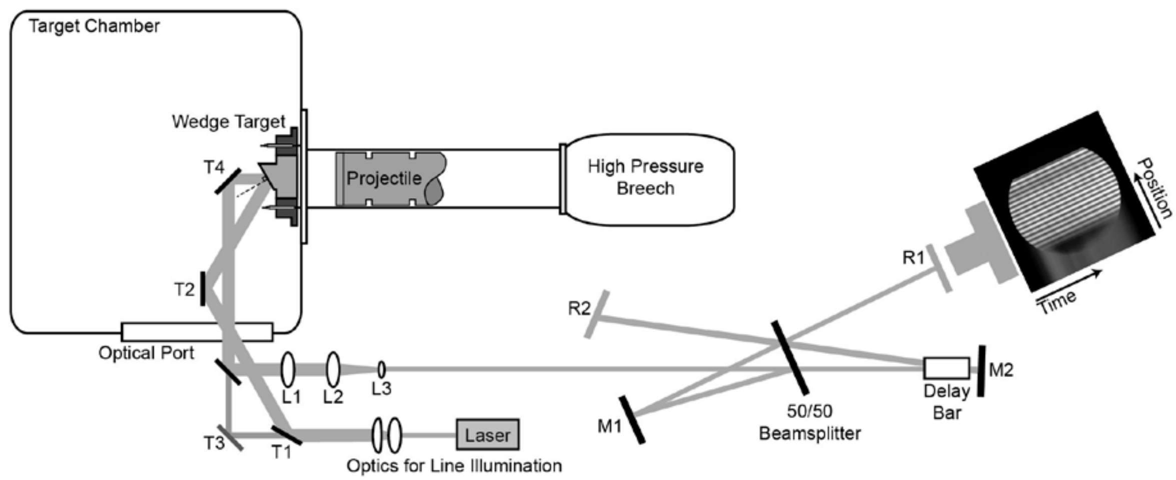

Figure 2. Illustration of ORVIS system coupled to a wedge-shaped gas gun target.

from 0.17-1.40 km/s. Our ORVIS system was previously coupled to the gas gun for investigations of the shock response of low-density granular materials [2,3] and the image analysis relies on a "rolling push-pull" method [3,4]. With this method, the intensity modulation data along lines parallel to the time axis of the streak camera are determined at the fringe center along with 1/4, 1/2, and 3/4 the distance to the center of the neighboring fringe and treated as the data recorded by four PMT channels in a "push-pull" VISAR [5].

The experimental arrangement of the ORVIS system coupled to the gas gun and a wedge-shaped target is given in Fig. 2. The coherent light from the source laser is confined to a thin line segment on the target by an arrangement of cylindrical and spherical lenses. Diffusely reflected light from the target is turned by a polarization-sensitive beamsplitter and collected by the first focusing lens (L1) and the telescope optics of L2 and L3 adjusts the image magnification for recording by the streak camera. The interferometer consists of a 50/50 beam splitter which splits the light into a reference leg and a delayed leg by passing through a fused silica delay bar. The observed motion of the interference fringes at the recombination plane (R1) is recorded at the streak camera slit and is directly proportional to target velocity.

When testing with planar targets, the source laser light completes two 90° turns with T3 and T4 and the collected light returns along the same path to the beam splitter and L1. For these wedge tests, the source laser light is directed onto the target at an angle to the wedge normal so that the centroid of the reflected light would fall on the path defined by the wedge to T4, the beam splitter and L1. Figure 2 illustrates the beam path for the 30° included angle of target B1 (Fig. 5).

DEMONSTRATION WITH BRASS WEDGES

Symmetric impact tests were conducted with brass wedges at a 0.6 km/s impact velocity. The location of the laser line on the target's inclined surface is shown in Fig. 3 and Fig. 4.

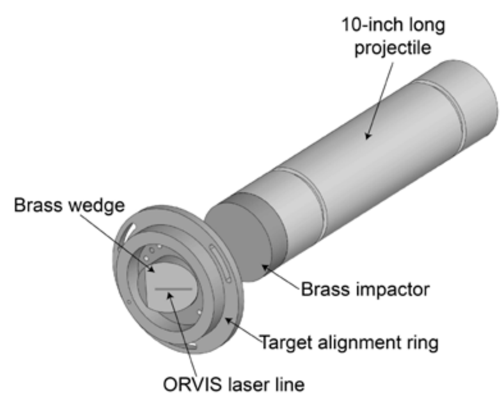

Figure 3. Illustration of wedge target and projectile.

During initial alignment of the beam (prior to installation of the line illumination optics), the location of the beam from the toe of the wedge was carefully measured along with the image magnification. This information determined the observation location along the wedge and enabled indexing the collected raw image data in time based on the spatial location where the first motion is observed. Similar to traditional wedge tests, the free surface motion of the wedge base was also monitored with a VISAR probe (only the fiber optic cable to the VISAR probe is visible to the left of the turning mirror T4 in the photo of Fig. 4).

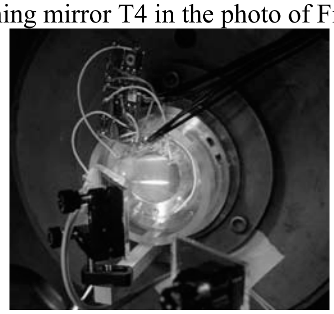

Figure 4. Photo of brass wedge target installed in the target chamber.

Data are presented here for two targets, B1 and B2, which differ in terms of the angle of the inclined surface and the thickness of the base cylinder (Fig. 5). These targets were machined from a single piece of brass; the diameter of the base equaled 6.86 cm and the diameter of the wedge equaled 4.08 cm. The surface of B1 was the as-machined surface (32 μin) whereas the surface of B2 was lightly polished with a diamond-grit polishing paper.

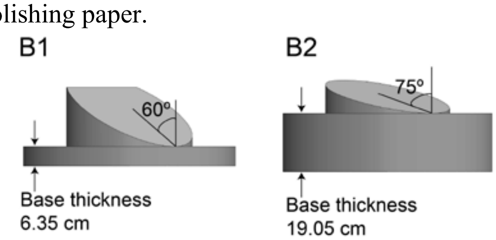

Figure 5. Details of the two brass wedge targets.

The maximum outer diameter of the base is fixed by the dimensions of the gas gun hardware. This forced the VISAR probe to be located near the outer edge such that the measured velocity was affected by the edge release waves. The data are given in Fig. 6 where the measured velocities from B2 (with the thicker base) were about half of the expected value of 0.6 km/s at the free surface. It is anticipated that stress gauges at the base-wedge interface will be implemented in future testing with explosive wedges due to the challenges of observing the free surface motion in the restricted available space.

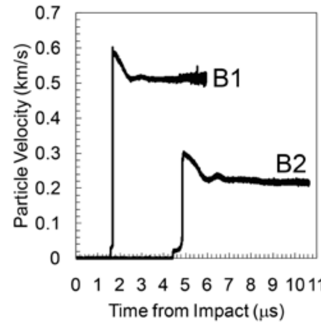

Figure 6. VISAR data from free surface of wedge base.

The raw image data for the two targets are given in Fig. 7. In both images, the interference fringes are stationary in time until the arrival of the elastic stress wave. Fringe motion is first observed at the bottom of each image (near the wedge toe). The slope of the disturbance in the raw image data correspond to the angle of the inclined target surface. Following the initial disturbance of the elastic wave is the plastic shock.

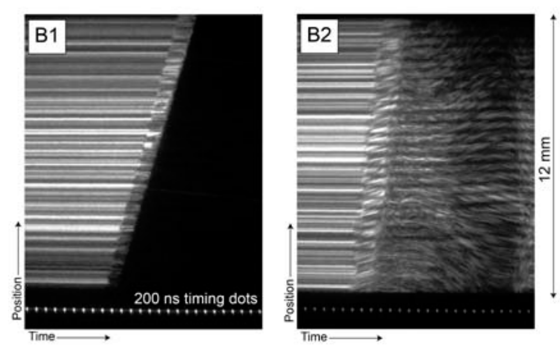

Figure 7. Raw image data for the two brass wedges.

After the plastic shock arrival, a loss of return light from B1 was observed as noted by a loss of fringe contrast. It is speculated that local changes in the surface roughness or orientation at the point of shock breakout directed the return light outside the collection pathway such that all signal was lost. The slope of the plastic wave disturbance in the raw image data was determined to equal 8.8 km/s and when corrected for the angle of the inclined surface, a measured shock velocity through the target of 4.4 km/s = 8.8 * sin 30° is calculate to be in good agreement of the shock velocity predicted by the brass Hugoniot [6] of 4.2 km/s. In the case of B2, the interference fringes were recorded well after the plastic shock arrival and variations in the surface motion are clearly evident.

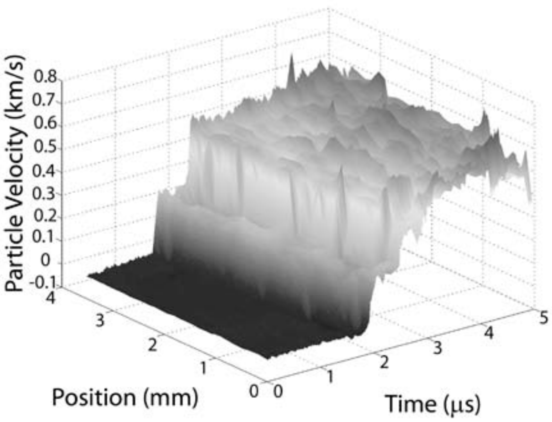

Figure 8. Surface plot of particle velocities from B2. The center 4 mm of image data is shown.

The raw image data can be post-processed into a surface plot of particle velocities as shown for B2 in Fig. 8. The particle velocity jumps due the elastic and plastic waves are visible. Additionally, the post-shock spatial and temporal variations of the inclined surface are also evident.

FUTURE WORK

The combination of our ORVIS diagnostic with a wedge test advances the capabilities of the traditional wedge test which only records the position-time shock path data. As Fig. 8 demonstrates, the post-shock variations provide significantly more data than previously possible. Our future efforts will apply this technique to explosive targets including machined wedges of Composition B and wedges of pressed explosive powders. It is expected that this experimental method will be able to observe the role of heterogeneities during the shock acceleration and detonation transition processes.

CONCLUSIONS

We have utilized our ORVIS diagnostic and gas gun facility to collect data on inclined surfaces. Thus, an Impact-Loaded Wedge Test capable of collecting the material particle velocities in addition to the standard shock path (distance-time data) has been developed. The concept has been demonstrated with brass wedges and ongoing work is conducting tests with explosive samples.

ACKNOWLEDGEMENTS

Sandia National Laboratories is a multi-program laboratory managed and operated by Sandia Corporation, a wholly owned subsidiary of Lockheed Martin Company, for the U.S. Department of Energy's National Nuclear Security Administration under Contract DE-AC04-94AL85000. Approved for public release, SAND2011-4917C.

REFERENCES

1. Dick, J.J., Forest, C.A., Ramsay, J.B., and Seitz, W.L., J. of Applied Physics, 63 (1988) 4881.
2. Trott, W.M., Baer, M.R., Castaneda, J.N., Chhabildas, L.C., and Asay, J.R., J. of Applied Physics, 101 (2007) 024917.
3. Trott, W.M., Knudson, M.D., Chhabildas, L.C., and Asay, J.R., in Shock Compression of Condensed Matter – 1999 (M. Furnish, et al. eds.), pp. 993-998.
4. Trott, W.M., Castaneda, J.N., O'Hare, J.J., Knudson, M.D., Chhabildas, L.C., Baer, M.R., and Asay, J.R., in Fundamental Issues and Applications of Shock-Wave and High-Strain-Rate Phenomena – 2001 (K. Staudhammer, et al. eds.), pp. 647-654.
5. W.F. Hemsing, Rev. Sci. Instrum., 50 (1979), 73.
6. Marsh, S.P., LASL Shock Hugoniot Data, Univ. of California Press, Berkeley, CA (1980).